



Published in final edited form as:

Eur J Pharmacol. 2018 June 05; 828: 9–17. doi:10.1016/j.ejphar.2018.02.045.

Protective effects of 7,8-dihydroxyflavone on neuropathological and neurochemical changes in a mouse model of Alzheimer's disease

Nurgul Aytan^{1,2,3,*}, Ji-Kyung Choi³, Isabel Carreras^{1,4}, Leah Crabtree^{1,2,5}, Brian Nguyen^{1,2}, Margaret Lehar^{1,2}, Jan Krzysztof Blusztajn⁶, Bruce G. Jenkins³, and Alpaslan Dedeoglu^{1,2,3}

¹Department of Veterans Affairs, VA Boston Healthcare System, Boston, MA 02130, USA

²Department of Neurology Boston University School of Medicine, Boston, MA 02118, USA

³Department of Radiology, Massachusetts General Hospital and Harvard Medical School, Boston, MA 02114, USA

⁴Department of Biochemistry Boston University School of Medicine, Boston, MA 02118, USA

⁵University of Exeter Medical School, Devon, EX4 4QJ, UK

⁶Department of Pathology Boston University School of Medicine, Boston, MA 02118, USA

Abstract

Interest in brain-derived neurotrophic factor (BDNF) was greatly enhanced when it was recognized that its expression is reduced in neurodegenerative disorders, especially in Alzheimer's disease (AD). BDNF signaling through the TrkB receptor has a central role in promoting synaptic transmission, synaptogenesis, and facilitating synaptic plasticity making the BDNF-TrkB signaling pathway an attractive candidate for targeted therapies.

Here we investigated the early effect of the small molecule TrkB agonist, 7,8 dihydroxyflavone (7,8-DHF), on AD-related pathology, dendritic arborization, synaptic density, and neurochemical changes in the 5xFAD mouse model of AD. We treated 5xFAD mice with 7,8-DHF for 2 months beginning at 1 month of age.

We found that, in this model of AD, 7,8-DHF treatment decreased cortical A β plaque deposition and protected cortical neurons against reduced dendritic arbor complexity but had no significant impact on the density of dendritic spines. In addition 7,8-DHF treatment protected against hippocampal increase in the level of choline-containing compounds and glutamate loss, but had no significant impact on hippocampal neurogenesis.

Keywords

Alzheimer's disease; 7; 8-Dihydroxyflavone; brain-derived neurotrophic factor (BDNF); choline

*Corresponding author: VA Boston Healthcare System, Research and Development Service, Building 1A - (151), 150 S. Huntington Avenue, Boston, MA 02130, USA. Tel: +1 857 364 6783 Fax: +1 857 364 4540.

Competing financial interests

The authors declare no competing financial interests.

1. Introduction

Alzheimer's disease (AD) is the most common age-related neurodegenerative disease, characterized by progressive memory loss and irreversible cognitive decline that correlates with the accumulation of extracellular senile plaques composed of amyloid β ($A\beta$) peptide and abnormalities in synaptic connectivity revealed by decreased dendritic arborization and dendritic spine loss in the hippocampus and cortex, the primary areas affected by AD-related pathology (DeKosky and Scheff, 1990; Selkoe, 2002; Terry et al., 1991).

Brain-derived neurotrophic factor (BDNF), one of the most abundant growth factors in the brain, is prominently involved in neuronal survival, synaptic transmission, and synaptic plasticity events underlying learning and memory through its interaction with the tropomyosin-related kinase B (TrkB) cellular receptor (Horch and Katz, 2002; Nagahara et al., 2009; Patterson et al., 1996). Clinical evidence suggests that a decrease in BDNF levels could be associated with the pathogenesis of AD. BDNF mRNA and protein expression are significantly reduced in the hippocampal and cortical areas of AD patients and decreased levels of serum BDNF have also been reported (Connor et al., 1997; Ferrer et al., 1999; Peng et al., 2005; Phillips et al., 1991). Additionally, a significant downregulation of TrkB expression in individual cholinergic neurons has been demonstrated during the progression of AD (Ginsberg et al., 2006). Reduced BDNF mRNA levels have been found to correlate with increased ratios of $A\beta_{42}/A\beta_{40}$ in transgenic mouse models of AD (Peng et al., 2009). Several studies have been conducted in animal models of AD to address the effect of therapeutic application of BDNF (Nagahara et al., 2013; Nagahara et al., 2009).

Due to the inability of BDNF to cross the blood brain barrier, efforts have been focused on identifying a small molecule that could mimic the neurotrophic effects of BDNF. Recently, 7,8-dihydroxyflavone (7,8-DHF), a naturally occurring flavone, was found to be a potent TrkB receptor agonist that mimics the action of BDNF downstream signaling (Jang et al., 2010). *In vivo* mouse studies showed that 7,8-DHF crosses the blood-brain barrier (Liu et al., 2013), and causes increased levels of phospho-TrkB protein in brain (Gao et al., 2016; Garcia-Diaz Barriga et al., 2017; Luo et al., 2016), consistent with the notion that it acts as BDNF analog and TrkB agonist. Ohno and Devi first reported that intraperitoneal (i.p.) injection of 7,8-DHF for 10 days in the 5xFAD mouse model at a late disease stage (12–15 months of age) reduces $A\beta$ levels, decreases β -secretase (BACE1), restores TrkB signaling and rescues memory impairment (Devi and Ohno, 2012). Subsequently, others confirmed and extended these findings using various AD mouse models (Bollen et al., 2013; Castello et al., 2014; Gao et al., 2016; Hsiao et al., 2014; Zhang et al., 2014b). Moreover, our studies indicate that 7,8-DHF has beneficial effects in a mouse model of amyotrophic lateral sclerosis (ALS) (Korkmaz et al., 2014) and others reported beneficial effects of 7,8-DHF in models of depression (Liu et al., 2010), Rett syndrome (Johnson et al., 2012), Parkinson's (Li et al., 2016; Luo et al., 2016; Sconce et al., 2015) and Huntington's (Jiang et al., 2013) diseases as well as amelioration of deficits in hippocampal neurogenesis in response to stress (Tzeng et al., 2013).

In this study, we sought to determine if 7,8-DHF will exhibit efficacy in preventing or slowing down the AD-related phenotypes in a transgenic mouse model of the disease. We

used 5xFAD mice, first developed by Oakley and colleagues (Oakley et al., 2006; Ohno et al., 2007), that coexpress human amyloid precursor protein (APP) and presenilin 1 (PS1) by combining multiple familial AD (FAD) mutations [APP K670N/M671L (Swedish) + I716V (Florida) + V717I (London) and PS1 M146L+ L286V]. These mice have been shown to develop cerebral amyloid plaques starting at 2 months of age and the abundance of plaques increase with age, reduced synaptic markers, neuronal loss, and memory impairment and are characterized by high ratio of brain A β 42/A β 40 peptide levels (Oakley et al., 2006; Ohno et al., 2007). These 5xFAD transgenic mice were treated with 7,8-DHF for 2 months beginning at 1 month of age before plaque deposition to determine if this early treatment can ameliorate neuropathological and neurochemical disease phenotypes. We specifically evaluated the effect of treatment on A β level and plaques, on neurogenesis, on dendritic morphology of cortical neurons, and on the neurochemical profile of the hippocampus. The latter was assessed with magnetic resonance spectroscopy (MRS) that can provide information on both neuronal viability using the marker N-acetylaspartate (NAA) and glial markers such as myo-inositol which are the neurochemical markers, increase in both AD mouse models (Choi et al., 2010a; Marjanska et al., 2005) as well as in humans (Pettegrew et al., 1997; Shonk et al., 1995). In addition to NAA and myo-inositol there are numerous other chemicals that can be measured including glutamate and glutamine, choline-containing compounds, scyllo-inositol, GABA and taurine (Choi et al., 2007).

We report that 7,8-DHF treatment reduced cortical A β plaque deposition, prevented the reduction of dendritic arborization of cortical neurons, protected against glutamate loss and the increase in the levels of choline-containing compounds in the hippocampus suggesting that 7,8-DHF treatment is a promising approach in AD therapy.

2. Material and Methods

2.1. Mice and treatment protocol

In this study, we used 5xFAD mice and non-transgenic littermates. 5xFAD transgenic mice coexpress human APP and PS1 with 5 familial AD (FAD) mutations [APP K670N/M671L (Swedish) + I716V (Florida) + V717I (London) and presenilin 1 (PS1) M146L+ L286V] with neuronal expression driven by the Thy-1 promoter. The initial breeders were purchased from Jackson Laboratory. Only female mice were used in the current study (n=10 mice per group). 5xFAD mice and WT littermates were treated with 7,8-dihydroxyflavone (Tocris Bioscience, Ellisville, MO, 5 mg/kg, 3 days a week by intraperitoneal (i.p) injection) for 2 months starting at 1 month of age. 7,8-dihydroxyflavone was dissolved in saline. In addition, a cohort of untreated 5xFAD mice (n=10) was used. All animal experiments were carried out in accordance with the NIH Guide for the Care and Use of Laboratory Animals and were approved by the local animal care committee. We monitored mice for general well-being, body weight and food and water consumption. Mice tolerated the treatment well with no effect on body weight or any other apparent adverse effects.

2.2. Tissue collection

At 3 months of age, mice (7,8-DHF-treated 5xFAD, non-transgenic mice (WT) and untreated-transgenic 5xFAD) were euthanized and brains removed for analysis. The left

hemisphere was post-fixed with 4 % paraformaldehyde solution for 24 h and cryoprotected in a graded series of 10% and 20% glycerol/2% DMSO solution for histological analysis. The right hemisphere was dissected using a 1mm mouse brain matrix. The prefrontal cortex (from bregma levels 3.2 to 1.3) was homogenized for the analysis of A β by enzyme-linked immunosorbent assay (ELISA) assays. The posterior hippocampus region (from bregma levels -2.7 to -3.7) was used to obtain a 1mm diameter punch for analysis of neurochemicals by MRS. The remaining brain tissue (from bregma levels 1.3 to -2.7) was processed for Golgi staining.

2.3. ELISA assay

The prefrontal cortex of the right hemibrain was homogenized with 5x volumes (w/v) of Tris-buffered saline (TBS) and centrifuged at 16,000 g for 1h at 4 °C. After removing the TBS-soluble fraction, the resulting pellet was resuspended with 8x cold 5M guanidine HCl buffer to analyze the insoluble A β content. To determine A β levels, human A β 40 and A β 42 ELISA kits (Invitrogen, Grand Island, NY) were used according to manufacturer's specifications. Briefly, TBS-soluble and insoluble samples were added into the wells of a 96-well plate and mixed with a cleavage-specific antibody to either A β 40 or A β 42. After overnight incubation at 4 °C, plates were washed and incubated with the secondary antibody for 30 min at 25 °C. The chromogenic substrate was added to the washed wells. The reaction was then stopped and color intensity was measured at 450 nm.

2.4. Histology/Immunohistochemistry

The cryoprotected hemibrain tissue was serially cut at 50 μ m on a freezing microtome. Serial sections of 500 μ m apart spanning the whole hemibrain were immunostained with antibodies to A β 1-40 and A β 1-42 (Invitrogen, Grand Island, NY #44348A, #44-344) to define A β deposits and to doublecortin (Cell Signaling Technology Inc., MA), as a marker of neurogenesis. Immunohistochemical procedures were performed as previously described (Kowall et al., 2000). In brief, free-floating sections were incubated overnight in primary antibody followed by PBS (Phosphate buffered saline) washes and incubation in peroxidase-conjugated secondary antibody followed by development using 3,3'-diaminobenzidine tetrahydrochloride (DAB) as a chromogen.

2.5. Quantitative analysis of A β deposits

For the estimation of A β plaque intensity, the cortex of three serial sections per mouse brain was analyzed blindly using a custom software written in Matlab. The most rostral section analyzed was at the anterior commissure level (~0.1 mm anterior to bregma), and each successive section was at 0.5mm increments caudal to the first. Stained histological sections were analyzed by taking digital images with Nikon Eclipse 80i microscope using an Optronics camera. Quantification was performed using a house-written Matlab program that processes JPEG pictures of the region of interest. Each image was normalized for color and brightness using an unaffected region of the section creating black and white images. The percentage of thresholded pixels to total pixels in the region of interest was calculated for each image and presented as the percentage of affected tissue.

2.6. Golgi-Cox staining

The right hemibrain tissue encompassing bregma levels 1.3 to -2.7 was stained using the FD Rapid GolgiStain kit (FD NeuroTechnologies, Inc., Catonsville, MD) following the manufacturer's protocol of the Golgi staining kit manual. The stained brain tissue was cut using a cryostat microtome (Leica Microsystems Inc., Buffalo Grove, IL) at 100- μ m-thickness and sections from bregma level 1.3 to -2.2 mm were mounted on gelatin-coated slides. Dendritic analyses were performed in the cortex region of 4 to 5 sections that were visualized at 60X magnification with an Olympus BX51 bright field microscope. The neurons were manually traced using NeuroLucida (MBF Bioscience, MicroBrightField Inc., Williston, VT). Dendritic spine density (number of spines/10 μ m of dendrite), total number of spines on dendrites per neuron, and Sholl analysis data were calculated using NeuroLucida Explorer 11. Sholl analysis shows the cumulative number of dendritic intersections at 10 μ m interval distance points starting from the cell body. The number of dendrites intersecting for each neuron cell was used as an index for total dendritic arborization. The data were fit using an asymmetric Gaussian line shape including full width half max, peak amplitude, peak distance and an asymmetry parameter (Buys T. S, 1972). The curve fits were compared using the R factor ratio test by varying the curve parameter (Hamilton, 1995).

2.7. Quantification of DCX positive cells

The dentate granule cell layer was contoured using a Nikon microscope at 20x magnification in combination with StereoInvestigator software (MicroBrightfield, Inc., Williston, VT, USA). Sections between bregma levels -2.46 and -2.80 mm were chosen for analyses using 3 sections per mouse separated by 500 μ m. A counting grid of 40x40 μ m was placed over the dentate granule cell layer. Using a 50x50 μ m counting frame DCX immunoreactive cells in the dentate gyrus were counted in randomly-placed sampling sites using 40x magnification.

2.8. High Resolution Magic Angle Spinning Spectroscopy (HRMAS)

In vitro magnetic resonance spectroscopy (MRS) was collected as previously published (Choi et al., 2010a; Choi et al., 2010b) using high resolution magic angle spinning (HRMAS) spectra on Bruker 14T (Billerica, MA). We obtained tissue punches of freshly frozen hippocampus tissue. The dissected tissue sample was placed into a glass cylinder positioned in a 3 mm zirconium oxide MAS rotor (volume 50 μ L). HRMAS measurements were performed using a sample spinning rate of 3.6 kHz selected to push the spinning side bands outside the frequency region of the metabolites. The experiments were performed at 4 °C to minimize tissue degradation. Data were acquired using a rotor synchronized, Carr-Purcell-Meiboom-Gill (CPMG) pulse sequence [$90 - (\tau - 180 - \tau - \text{Acq})_n$] with two different effective time to echo (TEs) of 100ms/10ms. The longer TE serves to remove the lipid/macromolecular resonances and the short TE retains them. The interpulse delay, τ , is synchronized to the rotor frequency, and is 272 μ s. The n value for the relatively short spin relaxation times (T_2) filter was 36 for the short TE and for the long TE was 360. The short τ value removes all the effective spin relaxation time (T_2^*) - like effects on the line shapes. The long T_2 filter yields approximately 95% of the total spectral intensity of all metabolites of interest compared to the short TE. Other acquisition parameters were a 90° pulse of 5-10 μ s, a spectral width of 8 kHz, 16K complex points, 256 averages and a TR of

5s. We also collected a water spectrum for each sample using the short TE CPMG sequence with a TR of 10s and 4 averages and no water suppression. Samples were placed in the rotor with a small amount of D₂O (Sigma-Aldrich, Milwaukee, WI) for locking and shimming.

The HRMAS spectra collected contain spectral information for a large number of neurochemicals (Choi et al. 2007). Data were analyzed using the Chenomx (Edmonton, Alberta, Canada) package fitting the entire metabolite spectrum for each neurochemical, using basis spectra from a large library of neurochemical including all the spin-spin couplings to minimize the residual difference between the observed and calculated spectrum. The spectra were fit for a total of 17 molecules including acetate, alanine, aspartate, cholines (phosphocholine, glycerophosphocholine, choline), gamma-amino-butyrate (GABA), glutamate, glutamine, glutathione, glycine, lactate, myo-inositol, *N*-acetylaspartate (NAA), *N*-acetylaspartylglutamate (NAAG), scyllo-inositol and taurine. The data are reported as molar ratios to creatine since our prior studies of the absolute concentrations in multiple different AD transgenic mouse models showed no change in total creatine between WT and any of the AD models (Choi et al., 2010a; Choi et al., 2010b; Dedeoglu et al., 2004). In a paper recently published by Mlynarik et al. 2012 (Mlynarik et al., 2012) examining the 5xFAD mice using a water normalization method, no significant change in the creatine concentrations were noted in the 5xFAD mice compared to WT. Classification of the data was performed using Weka (Mark Hall, 2009).

2.9. Data analyses

Statistical analyses of the data were performed using a one-way ANOVA with Tukey HSD post-hoc tests.

3. Results

3.1. Effect of 7,8-DHF treatment on A β 42 and A β 40 levels

We evaluated the effect of 7,8-DHF treatment on TBS-soluble and insoluble A β 42 and A β 40 levels by ELISA in the prefrontal cortex. In the TBS soluble fraction, A β 40 and A β 42 were below the detectable level of the kits. Consistent with our previous studies using 5xFAD mice, the cortical levels of insoluble A β 42 were higher than those of A β 40 (Aytan et al., 2016; Aytan et al., 2013; Kantarci et al., 2017). Although 7,8-DHF-treated 5xFAD mice exhibited a decrease in the levels of insoluble A β 42 and A β 40 compared to untreated transgenic littermates, this trend was not statistically significant (Fig 1).

3.2. Effect of 7,8-DHF treatment on A β plaque load

We investigated the impact of 7,8-DHF administration on amyloid plaque deposition in the frontal cortex of 3 month-old 5xFAD mice. Since relative changes in A β 42:A β 40 ratio towards elevated A β 42, the more pathogenic form, is critical to AD we immunostained A β plaques with specific antibodies to A β 40 and A β 42. We found that 7,8-DHF treatment significantly decreased A β 42 plaque deposition while the change in A β 40 deposition was not statistically significant (Fig 2).

3.3. Effect of 7,8-DHF treatment on dendritic length, arborization and spine density

To determine the effect of 7,8-DHF treatment on the quantity of dendritic spines and dendritic arborization, we counted spines and dendrites on the cortical layer V pyramidal neurons of untreated wild type (WT) and 5xFAD mice at 3 months of age. Spine density and total spine number per neuron (n=5 neurons/mouse) were quantified and analyzed on dendritic branch orders 2 and 3 for each animal (n=6) (Fig 3A). Spine density and total spine number were significantly lower in untreated 5xFAD mice compared to WT mice. 7,8-DHF treatment appear to prevent this AD-model-related loss of spine density and total spine number on the dendritic branch orders 2 and 3 since the spine number and density in 7,8-DHF treated-5xFAD mice are no longer significantly different than those of WT mice (Fig 3B and 3C).

The numbers of dendritic intersections for each neuron within each 10 μm segment (radial distance) from the soma of neurons were computed and dendritic arborization was evaluated using Sholl analysis for the groups. The analysis revealed that the pruning of the dendritic tree that characterizes the 5xFAD mice as compared to WT animals was prevented by 7,8-DHF treatment (Fig 3D).

3.4. Effect 7,8-DHF treatment on doublecortin (DCX) positive cells

We investigated the effect of 7,8-DHF treatment on neurogenesis in 5xFAD mice. As expected the number of DCX-positive cells was lower in the 5xFAD mice as compared to the WT littermates. 7,8-DHF treated 5xFAD mice had a slightly higher number of DCX-stained cells than the controls, however this difference was not statistically significant (Fig 4).

3.5. Magnetic resonance spectroscopy of changes in brain neurochemicals

As we have reported previously, we found very small neurochemical changes between 5xFAD and WT animals at 3 months of age, although there are huge changes at 8 months of age (Aytan et al., 2016; Aytan et al., 2013). Similar to results we found previously at 3 months of age, there is a small (ca. 10%) decrease in glutamate levels (5xFAD = 0.98 ± 0.06 ; 5xFAD +7,8-DHF = 1.11 ± 0.1 ; WT = 1.1 ± 0.08 ; $F_{25,2} = 6.88$; $p < 0.0046$) in the 5xFAD mice compared to WT animals that was prevented by the treatment with 7,8-DHF (Fig 5 and Fig 6).

We quantified the various choline-containing compounds from the three major resonances: glycerophosphocholine (GPC; 3.24 ppm), phosphocholine (PhC; 3.23 ppm) and choline (Cho; 3.2 ppm). We found that there was an increase in Cho and PhC intensity in the 5xFAD mice compared to WT animals, that like the decrease in glutamate was also prevented by the DHF treatment. The results for the choline-containing compounds were as follows: PhC (WT = 0.148 ± 0.026 ; 5xFAD = 0.16 ± 0.022 ; 5xFAD + 7,8-DHF = 0.128 ± 0.013 ; $F_{25,2} = 4.79$; $p = 0.007$); Cho (WT = 0.183 ± 0.027 ; 5xFAD = 0.236 ± 0.042 ; 5xFAD +7,8-DHF = 0.171 ± 0.036 ; $F_{25,2} = 8.12$; $p = 0.00215$). There was no significant change in the GPC levels ($F_{25,2} = 0.51$; $p = 0.6$) between the three groups of animals.

4. Discussion

In this study, we sought to determine whether 7,8-DHF treatment has a significant positive impact on several measures of brain pathology when administered before the onset of amyloid plaque deposition in the 5xFAD AD mouse model. 5xFAD mice develop amyloid plaques in the cortex and hippocampus starting at 2 months of age and display significant impairment in their working memory by 4–5 months of age (Oakley et al., 2006). Therefore animals were treated with 7,8-DHF starting at 1 month of age for 2 months.

Ohno and Devi reported reduced A β peptide levels, restored TrkB signaling and rescued memory impairment following i.p. injection of 7,8-DHF for 10 days in the 5xFAD mouse model at 12–15 months of age (Devi and Ohno, 2012). Consistent with its expected mechanism of action as a TrkB agonist, systemic administration of 7,8-DHF in that study significantly rescued the decline in phospho-TrkB levels without affecting total TrkB protein expression. In both WT and 5xFAD mice, Devi and Ohno (2012) also observed the 7,8-DHF-evoked downregulation of expression of the beta-secretase (BACE) enzyme that catalyzes the initial step in the production of both A β 40 and A β 42. They postulated that the amelioration of amyloid deposition by 7,8-DHF in 5xFAD mice may be mediated by this reduction of BACE activity. It is likely that this mechanism was also responsible for the anti-amyloidogenic actions of 7,8-DHF observed in this study. It is worth noting that while the 7,8-DHF treatment was associated with the average reduction of all measures of amyloidosis performed here (tissue A β 40 and A β 42 peptide levels assayed by ELISA as well as A β 40 and A β 42 plaque deposition assessed by immunohistochemical staining), only the latter effect was statistically significant with the number of subjects available for analyses. We attribute this to the possibility that A β 42 plaques are particularly stable and thus subjects to lower individual variability than that observed for the other measures that exhibited higher variance. The high variance of these measures would also be expected in our relatively young 3-month old mice that are at early stages of disease. Our data are consistent with the results reported by Zhang et al (Zhang et al., 2014b) who observed reduced numbers of amyloid plaques in hippocampi of 5xFAD mice chronically treated with 7,8-DHS between the ages of 2 to 6 months with no changes of A β 42 levels. These authors (Zhang et al., 2014b) also reported the neuroprotective effects of 7,8-DHF treatment on A β -induced toxicity in primary cortical neurons and the promotion of dendritic growth and synaptogenesis in primary cortical neuron culture, loss of hippocampal synapses, synaptic dysfunction, and memory deficits. Dendritic spine loss is observed in the hippocampus and cortex of the brains of individuals with AD (DeKosky and Scheff, 1990; Walsh and Selkoe, 2004). Our results are consistent with these clinical data: untreated 5xFAD mice had reduced dendritic spine density and dendritic arborization compared to WT mice at 3 months of age. A previous study had demonstrated that 7,8-DHF treatment in mice with experimental cortical and hippocampal neuronal death significantly increased thin spine density (Castello et al., 2014). In our study, we observed a similar trend for 7,8-DHF treatment to increase spine density on the dendrites of cortical neurons. Moreover, in this study 7,8-DHF treatment prevented the loss of hippocampal pyramidal neuron dendritic arbor complexity seen in 5xFAD mice. Thus, in addition to preventing amyloidosis, 7,8-DHF may act on the pyramidal neuron to protect them from the toxic actions of A β peptides. It is worth noting

that 7,8-DHF is effective in supporting dendritic spines and arborization in models of other neural diseases (Korkmaz et al., 2014; Stagni et al., 2017; Tian et al., 2015; Zeng et al., 2012; Zhang et al., 2014a), suggesting that these trophic actions of the TrkB agonist are of general nature.

We and others previously found, that there are profound changes in the brain metabolites of 5xFAD mice compared to controls at 8 months of age (Aytan et al., 2016; Aytan et al., 2013; Mlynarik et al., 2012). Similar to what we and others have found in other AD mouse models including the triple transgenic model (Aytan et al., 2013; Choi et al., 2010a; Choi et al., 2007; Choi et al., 2010b; Dedeoglu et al., 2004; Marjanska et al., 2005), there are many similar changes in AD mouse models and humans with AD, including decreased NAA and glutamate levels and increased levels of myo-inositol, taurine, glutamine and choline-containing compounds. While many of the changes are age-dependent, the later stages in all the models show great similarities. We earlier showed that there were large changes in brain neurochemicals in 5xFAD mice between the ages of 3 and 8 month old (Aytan et al., 2013). The only change in neurochemicals that we have reported in 3 month old 5xFAD mice was a small, but significant, decrease in glutamate concentration. We have now replicated the decrease in glutamate in 3 month old 5xFAD mice and found that the glutamate loss is protected by 7,8-DHF treatment (see Fig 6).

Also new to this study is the more precise identification of choline-containing resonances showing that there are increases in total choline (at 3.20 ppm) and smaller increases in phosphocholine (3.23 ppm) but not in glycerophosphocholine (3.24 ppm) levels in the hippocampus of 5xFAD mice as compared to WT. Importantly, 7,8-DHF treatment prevented the increase in choline levels. Increased Cho/Cr ratio has been previously reported in patients with AD (Bartha et al., 2008). Choline is the rate-limiting precursor to acetylcholine and phosphatidylcholine. When neurons are deprived of choline they will catabolize membranes and use the choline for acetylcholine (Ach) synthesis (Lee et al., 1993; Zhao et al., 2001). Therefore, there is some evidence that loss of cholinergic function in AD may produce increased membrane-free choline (Miller, 1991). Increased Cho/Cr ratio has been previously reported in patients with AD (Bartha et al., 2008) suggesting increased membrane turnover and phosphatidylcholine catabolism.

Increases in PhC, GPC and Cho are found in AD cerebrospinal fluid (CSF) compared to normal controls (Walter et al., 2004). While increases in choline-containing compounds have been observed often in human AD MRS studies (with a review and meta-analysis published by Tumati et al. (Tumati et al., 2013)), it is difficult in human *in vivo* studies to separate PhC, GPC and Cho due to lower field strengths and larger linewidths in the *in vivo* studies. Here, using *in vitro* MRS with HRMAS we are able to readily separate the three choline-containing components and it is clear that most of the increase noted at 3 months of age in 5xFAD mice is occurring in the Cho resonance at 3.2 ppm. Studies of multiple diseases leading to inflammation such as multiple sclerosis and HIV infection show large increases in choline levels during inflammatory stages of the lesions (Chang et al., 2013). This may reflect early damage to membranes or increased membrane turnover. The putative mechanism is elevated intracellular Ca^{++} concentration that leads to activation of phospholipase A and degradation of phosphatidylcholine into GPC and free choline (Chang

et al., 2013; Miller, 1991; Walter et al., 2004). In any case, the MRS provides data that is supportive of the protective role of 7,8-DHF, likely through TrkB downstream mechanisms.

5. Conclusion

In conclusion, our study shows that 7,8-DHF treatment of 5xFAD mice at the earliest stages of AD-like pathology prevents and/or delays several pathophysiologic processes associated with this disease. The study supports the idea that preventive interventions in AD with the use of natural products are viable and that the BDNF/TrkB signaling pathway is a rational target for those.

Acknowledgments

This research is supported by grants from the Department of Veteran Affairs (Merit Award) to A. Dedeoglu and NIH grant AG045031 to JKB.

References

- Aytan N, Choi JK, Carreras I, Brinkmann V, Kowall NW, Jenkins BG, Dedeoglu A. Fingolimod modulates multiple neuroinflammatory markers in a mouse model of Alzheimer's disease. *Sci Rep.* 2016; 6:24939. [PubMed: 27117087]
- Aytan N, Choi JK, Carreras I, Kowall NW, Jenkins BG, Dedeoglu A. Combination therapy in a transgenic model of Alzheimer's disease. *Exp Neurol.* 2013; 250:228–238. [PubMed: 24120437]
- Bartha R, Smith M, Rupsingh R, Rylett J, Wells JL, Borrie MJ. High field (1)H MRS of the hippocampus after donepezil treatment in Alzheimer disease. *Prog Neuropsychopharmacol Biol Psychiatry.* 2008; 32:786–793. [PubMed: 18252268]
- Bollen E, Vanmierlo T, Akkerman S, Wouters C, Steinbusch HM, Prickaerts J. 7,8-Dihydroxyflavone improves memory consolidation processes in rats and mice. *Behavioural brain research.* 2013; 257:8–12. [PubMed: 24070857]
- Buyts TS, aDCK. Bi-Gaussian fitting of skewed peaks. *Anal Chem.* 1972; 44:1273–1275.
- Castello NA, Nguyen MH, Tran JD, Cheng D, Green KN, LaFerla FM. 7,8-Dihydroxyflavone, a small molecule TrkB agonist, improves spatial memory and increases thin spine density in a mouse model of Alzheimer disease-like neuronal loss. *PloS one.* 2014; 9:e91453. [PubMed: 24614170]
- Chang L, Munsaka SM, Kraft-Terry S, Ernst T. Magnetic resonance spectroscopy to assess neuroinflammation and neuropathic pain. *J Neuroimmune Pharmacol.* 2013; 8:576–593. [PubMed: 23666436]
- Choi JK, Carreras I, Dedeoglu A, Jenkins BG. Detection of increased scyllo-inositol in brain with magnetic resonance spectroscopy after dietary supplementation in Alzheimer's disease mouse models. *Neuropharmacology.* 2010a; 59:353–357. [PubMed: 20399219]
- Choi JK, Dedeoglu A, Jenkins BG. Application of MRS to mouse models of neurodegenerative illness. *NMR Biomed.* 2007; 20:216–237. [PubMed: 17451183]
- Choi JK, Jenkins BG, Carreras I, Kaymakcalan S, Cormier K, Kowall NW, Dedeoglu A. Anti-inflammatory treatment in AD mice protects against neuronal pathology. *Exp Neurol.* 2010b; 223:377–384. [PubMed: 19679126]
- Connor B, Young D, Yan Q, Faull RL, Synek B, Dragunow M. Brain-derived neurotrophic factor is reduced in Alzheimer's disease. *Brain Res Mol Brain Res.* 1997; 49:71–81. [PubMed: 9387865]
- Dedeoglu A, Choi JK, Cormier K, Kowall NW, Jenkins BG. Magnetic resonance spectroscopic analysis of Alzheimer's disease mouse brain that express mutant human APP shows altered neurochemical profile. *Brain research.* 2004; 1012:60–65. [PubMed: 15158161]
- DeKosky ST, Scheff SW. Synapse loss in frontal cortex biopsies in Alzheimer's disease: correlation with cognitive severity. *Ann Neurol.* 1990; 27:457–464. [PubMed: 2360787]

- Devi L, Ohno M. 7,8-dihydroxyflavone, a small-molecule TrkB agonist, reverses memory deficits and BACE1 elevation in a mouse model of Alzheimer's disease. *Neuropsychopharmacology*. 2012; 37:434–444. [PubMed: 21900882]
- Ferrer I, Marin C, Rey MJ, Ribalta T, Goutan E, Blanco R, Tolosa E, Marti E. BDNF and full-length and truncated TrkB expression in Alzheimer disease. Implications in therapeutic strategies. *J Neuropathol Exp Neurol*. 1999; 58:729–739. [PubMed: 10411343]
- Gao L, Tian M, Zhao HY, Xu QQ, Huang YM, Si QC, Tian Q, Wu QM, Hu XM, Sun LB, McClintock SM, Zeng Y. TrkB activation by 7, 8-dihydroxyflavone increases synapse AMPA subunits and ameliorates spatial memory deficits in a mouse model of Alzheimer's disease. *J Neurochem*. 2016; 136:620–636. [PubMed: 26577931]
- Garcia-Diaz Barriga G, Giralta A, Anglada-Huguet M, Gaja-Capdevila N, Orlandi JG, Soriano J, Canals JM, Alberch J. 7,8-dihydroxyflavone ameliorates cognitive and motor deficits in a Huntington's disease mouse model through specific activation of the PLCgamma1 pathway. *Human molecular genetics*. 2017; 26:3144–3160. [PubMed: 28541476]
- Ginsberg SD, Che S, Wu J, Counts SE, Mufson EJ. Down regulation of trk but not p75NTR gene expression in single cholinergic basal forebrain neurons mark the progression of Alzheimer's disease. *J Neurochem*. 2006; 97:475–487. [PubMed: 16539663]
- Hamilton W. Significance tests on the crystallographic R factor. *Acta Crystal*. 1995; 18:502–510.
- Horch HW, Katz LC. BDNF release from single cells elicits local dendritic growth in nearby neurons. *Nat Neurosci*. 2002; 5:1177–1184. [PubMed: 12368805]
- Hsiao YH, Hung HC, Chen SH, Gean PW. Social interaction rescues memory deficit in an animal model of Alzheimer's disease by increasing BDNF-dependent hippocampal neurogenesis. *J Neurosci*. 2014; 34:16207–16219. [PubMed: 25471562]
- Jacobsen JS, Wu CC, Redwine JM, Comery TA, Arias R, Bowlby M, Martone R, Morrison JH, Pangalos MN, Reinhart PH, Bloom FE. Early-onset behavioral and synaptic deficits in a mouse model of Alzheimer's disease. *Proc Natl Acad Sci U S A*. 2006; 103:5161–5166. [PubMed: 16549764]
- Jang SW, Liu X, Yepes M, Shepherd KR, Miller GW, Liu Y, Wilson WD, Xiao G, Blanchi B, Sun YE, Ye K. A selective TrkB agonist with potent neurotrophic activities by 7,8-dihydroxyflavone. *Proc Natl Acad Sci U S A*. 2010; 107:2687–2692. [PubMed: 20133810]
- Jiang M, Peng Q, Liu X, Jin J, Hou Z, Zhang J, Mori S, Ross CA, Ye K, Duan W. Small-molecule TrkB receptor agonists improve motor function and extend survival in a mouse model of Huntington's disease. *Human molecular genetics*. 2013; 22:2462–2470. [PubMed: 23446639]
- Johnson RA, Lam M, Punzo AM, Li H, Lin BR, Ye K, Mitchell GS, Chang Q. 7,8-dihydroxyflavone exhibits therapeutic efficacy in a mouse model of Rett syndrome. *J Appl Physiol*. 2012; 112:704–710. [PubMed: 22194327]
- Kantarci A, Aytan N, Palaska I, Stephens D, Crabtree L, Benincasa C, Jenkins BG, Carreras I, Dedeoglu A. Combined administration of resolvin E1 and lipoxin A4 resolves inflammation in a murine model of Alzheimer's disease. *Exp Neurol*. 2017; 300:111–120. [PubMed: 29126887]
- Korkmaz OT, Aytan N, Carreras I, Choi JK, Kowall NW, Jenkins BG, Dedeoglu A. 7,8-Dihydroxyflavone improves motor performance and enhances lower motor neuronal survival in a mouse model of amyotrophic lateral sclerosis. *Neuroscience letters*. 2014; 566:286–291. [PubMed: 24637017]
- Kowall NW, Hantraye P, Brouillet E, Beal MF, McKee AC, Ferrante RJ. MPTP induces alpha-synuclein aggregation in the substantia nigra of baboons. *Neuroreport*. 2000; 11:211–213. [PubMed: 10683860]
- Lee HC, Fellenz-Maloney MP, Liscovitch M, Blusztajn JK. Phospholipase D-catalyzed hydrolysis of phosphatidylcholine provides the choline precursor for acetylcholine synthesis in a human neuronal cell line. *Proc Natl Acad Sci USA*. 1993; 90:10086–10090. [PubMed: 8234260]
- Li XH, Dai CF, Chen L, Zhou WT, Han HL, Dong ZF. 7,8-dihydroxyflavone Ameliorates Motor Deficits Via Suppressing alpha-synuclein Expression and Oxidative Stress in the MPTP-induced Mouse Model of Parkinson's Disease. *CNS Neurosci Ther*. 2016; 22:617–624. [PubMed: 27079181]

- Liu X, Chan CB, Jang SW, Pradoldej S, Huang J, He K, Phun LH, France S, Xiao G, Jia Y, Luo HR, Ye K. A Synthetic 7, 8-Dihydroxyflavone Derivative Promotes Neurogenesis and Exhibits Potent Antidepressant Effect. *J Med Chem.* 2010
- Liu X, Qi Q, Xiao G, Li J, Luo HR, Ye K. O-methylated metabolite of 7,8-dihydroxyflavone activates TrkB receptor and displays antidepressant activity. *Pharmacology.* 2013; 91:185–200. [PubMed: 23445871]
- Luo D, Shi Y, Wang J, Lin Q, Sun Y, Ye K, Yan Q, Zhang H. 7,8-dihydroxyflavone protects 6-OHDA and MPTP induced dopaminergic neurons degeneration through activation of TrkB in rodents. *Neuroscience letters.* 2016; 620:43–49. [PubMed: 27019033]
- Marjanska M, Curran GL, Wengenack TM, Henry PG, Bliss RL, Poduslo JF, Jack CR Jr, Ugurbil K, Garwood M. Monitoring disease progression in transgenic mouse models of Alzheimer's disease with proton magnetic resonance spectroscopy. *Proc Natl Acad Sci U S A.* 2005; 102:11906–11910. [PubMed: 16091461]
- Mark Hall, EF., Holmes, Geoffrey, Pfahringer, Bernhard, Reutemann, Peter, Witten, Ian H. *The WEKA Data Mining Software: An Update; SIGKDD Explorations.* 2009. p. 11
- Miller BL. A review of chemical issues in 1H NMR spectroscopy: N-acetyl-L-aspartate, creatine and choline. *NMR Biomed.* 1991; 4:47–52.
- Mlynarik V, Cacquevel M, Sun-Reimer L, Janssens S, Cudalbu C, Lei H, Schneider BL, Aebischer P, Gruetter R. Proton and phosphorus magnetic resonance spectroscopy of a mouse model of Alzheimer's disease. *J Alzheimers Dis.* 2012; 31(Suppl 3):S87–99. [PubMed: 22451319]
- Nagahara AH, Mateling M, Kovacs I, Wang L, Eggert S, Rockenstein E, Koo EH, Masliah E, Tuszynski MH. Early BDNF Treatment Ameliorates Cell Loss in the Entorhinal Cortex of APP Transgenic Mice. *J Neurosci.* 2013; 33:15596–15602. [PubMed: 24068826]
- Nagahara AH, Merrill DA, Coppola G, Tsukada S, Schroeder BE, Shaked GM, Wang L, Blesch A, Kim A, Conner JM, Rockenstein E, Chao MV, Koo EH, Geschwind D, Masliah E, Chiba AA, Tuszynski MH. Neuroprotective effects of brain-derived neurotrophic factor in rodent and primate models of Alzheimer's disease. *Nat Med.* 2009; 15:331–337. [PubMed: 19198615]
- Oakley H, Cole SL, Logan S, Maus E, Shao P, Craft J, Guillozet-Bongaarts A, Ohno M, Disterhoft J, Van Eldik L, Berry R, Vassar R. Intra-neuronal beta-amyloid aggregates, neurodegeneration, and neuron loss in transgenic mice with five familial Alzheimer's disease mutations: potential factors in amyloid plaque formation. *J Neurosci.* 2006; 26:10129–10140. [PubMed: 17021169]
- Ohno M, Cole SL, Yasvoina M, Zhao J, Citron M, Berry R, Disterhoft JF, Vassar R. BACE1 gene deletion prevents neuron loss and memory deficits in 5XFAD APP/PS1 transgenic mice. *Neurobiol Dis.* 2007; 26:134–145. [PubMed: 17258906]
- Patterson SL, Abel T, Deuel TA, Martin KC, Rose JC, Kandel ER. Recombinant BDNF rescues deficits in basal synaptic transmission and hippocampal LTP in BDNF knockout mice. *Neuron.* 1996; 16:1137–1145. [PubMed: 8663990]
- Peng S, Garzon DJ, Marchese M, Klein W, Ginsberg SD, Francis BM, Mount HT, Mufson EJ, Salehi A, Fahnestock M. Decreased brain-derived neurotrophic factor depends on amyloid aggregation state in transgenic mouse models of Alzheimer's disease. *J Neurosci.* 2009; 29:9321–9329. [PubMed: 19625522]
- Peng S, Wu J, Mufson EJ, Fahnestock M. Precursor form of brain-derived neurotrophic factor and mature brain-derived neurotrophic factor are decreased in the pre-clinical stages of Alzheimer's disease. *J Neurochem.* 2005; 93:1412–1421. [PubMed: 15935057]
- Pettegrew JW, Klunk WE, Panchalingam K, McClure RJ, Stanley JA. Magnetic resonance spectroscopic changes in Alzheimer's disease. *Ann N Y Acad Sci.* 1997; 826:282–306. [PubMed: 9329700]
- Phillips HS, Hains JM, Armanini M, Laramee GR, Johnson SA, Winslow JW. BDNF mRNA is decreased in the hippocampus of individuals with Alzheimer's disease. *Neuron.* 1991; 7:695–702. [PubMed: 1742020]
- Sconce MD, Churchill MJ, Moore C, Meshul CK. Intervention with 7,8-dihydroxyflavone blocks further striatal terminal loss and restores motor deficits in a progressive mouse model of Parkinson's disease. *Neuroscience.* 2015; 290:454–471. [PubMed: 25655214]

- Selkoe DJ. Alzheimer's disease is a synaptic failure. *Science*. 2002; 298:789–791. [PubMed: 12399581]
- Selkoe DJ, Hardy J. The amyloid hypothesis of Alzheimer's disease at 25 years. *EMBO Mol Med*. 2016; 8:595–608. [PubMed: 27025652]
- Shonk TK, Moats RA, Gifford P, Michaelis T, Mandigo JC, Izumi J, Ross BD. Probable Alzheimer disease: diagnosis with proton MR spectroscopy. *Radiology*. 1995; 195:65–72. [PubMed: 7892497]
- Stagni F, Giacomini A, Guidi S, Emili M, Uguagliati B, Salvalai ME, Bortolotto V, Grilli M, Rimondini R, Bartesaghi R. A flavonoid agonist of the TrkB receptor for BDNF improves hippocampal neurogenesis and hippocampus-dependent memory in the Ts65Dn mouse model of DS. *Exp Neurol*. 2017; 298:79–96. [PubMed: 28882412]
- Terry RD, Masliah E, Salmon DP, Butters N, DeTeresa R, Hill R, Hansen LA, Katzman R. Physical basis of cognitive alterations in Alzheimer's disease: synapse loss is the major correlate of cognitive impairment. *Ann Neurol*. 1991; 30:572–580. [PubMed: 1789684]
- Tian M, Zeng Y, Hu Y, Yuan X, Liu S, Li J, Lu P, Sun Y, Gao L, Fu D, Li Y, Wang S, McClintock SM. 7, 8-Dihydroxyflavone induces synapse expression of AMPA GluA1 and ameliorates cognitive and spine abnormalities in a mouse model of fragile X syndrome. *Neuropharmacology*. 2015; 89:43–53. [PubMed: 25229717]
- Tumati S, Martens S, Aleman A. Magnetic resonance spectroscopy in mild cognitive impairment: systematic review and meta-analysis. *Neurosci Biobehav Rev*. 2013; 37:2571–2586. [PubMed: 23969177]
- Tzeng WY, Chuang JY, Lin LC, Cherng CG, Lin KY, Chen LH, Su CC, Yu L. Companions reverse stressor-induced decreases in neurogenesis and cocaine conditioning possibly by restoring BDNF and NGF levels in dentate gyrus. *Psychoneuroendocrinology*. 2013; 38:425–437. [PubMed: 22832183]
- Walsh DM, Selkoe DJ. Deciphering the molecular basis of memory failure in Alzheimer's disease. *Neuron*. 2004; 44:181–193. [PubMed: 15450169]
- Walter A, Korth U, Hilgert M, Hartmann J, Weichel O, Hilgert M, Fassbender K, Schmitt A, Klein J. Glycerophosphocholine is elevated in cerebrospinal fluid of Alzheimer patients. *Neurobiol Aging*. 2004; 25:1299–1303. [PubMed: 15465626]
- Zeng Y, Lv F, Li L, Yu H, Dong M, Fu Q. 7,8-dihydroxyflavone rescues spatial memory and synaptic plasticity in cognitively impaired aged rats. *J Neurochem*. 2012; 122:800–811. [PubMed: 22694088]
- Zhang JC, Wu J, Fujita Y, Yao W, Ren Q, Yang C, Li SX, Shirayama Y, Hashimoto K. Antidepressant effects of TrkB ligands on depression-like behavior and dendritic changes in mice after inflammation. *Int J Neuropsychopharmacol*. 2014a:18.
- Zhang Z, Liu X, Schroeder JP, Chan CB, Song M, Yu SP, Weinshenker D, Ye K. 7,8-dihydroxyflavone prevents synaptic loss and memory deficits in a mouse model of Alzheimer's disease. *Neuropsychopharmacology*. 2014b; 39:638–650. [PubMed: 24022672]
- Zhao D, Frohman MA, Blusztajn JK. Generation of choline for acetylcholine synthesis by phospholipase D isoforms. *BMC Neurosci*. 2001; 2:16. [PubMed: 11734063]

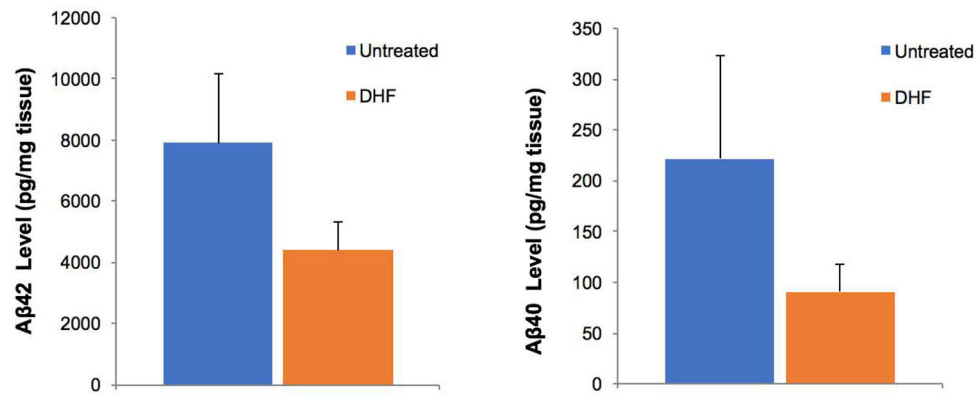


Fig 1. Concentration of total Aβ42 and Aβ40 levels were measured by ELISA in the prefrontal cortex. The decrease in the levels of Aβ42 and 40 in the 7,8 DHF 5xFAD treated group (n=10) was not statistically significant compared to the levels in untreated-5xFAD mice (n=10).

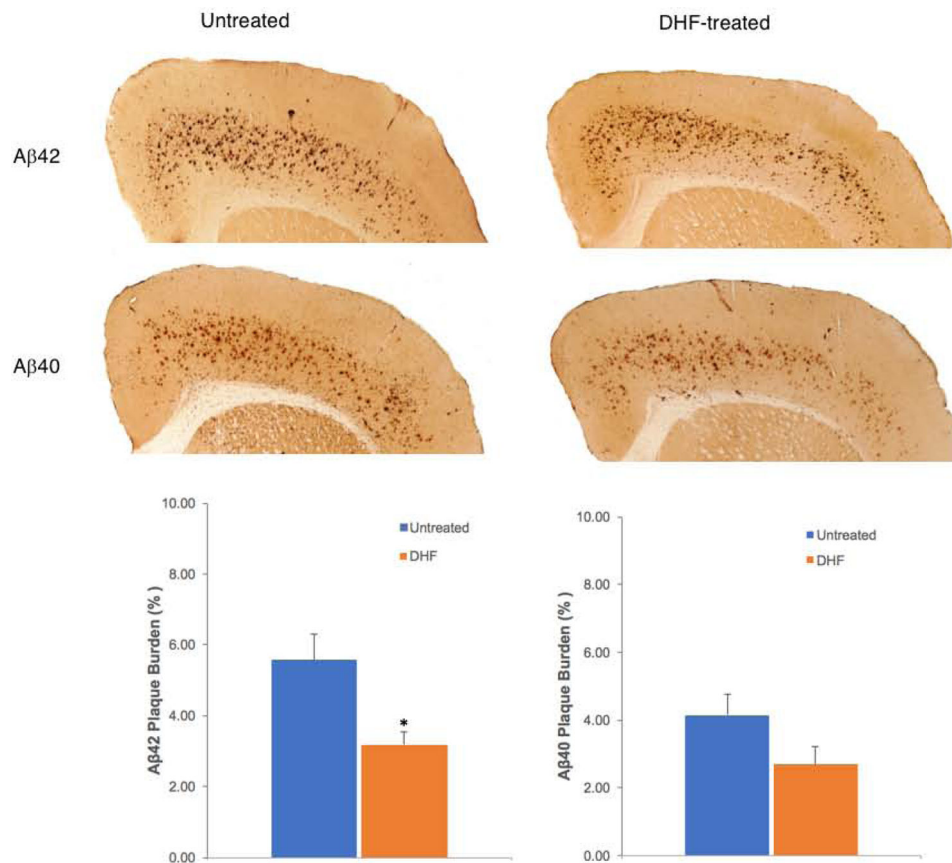
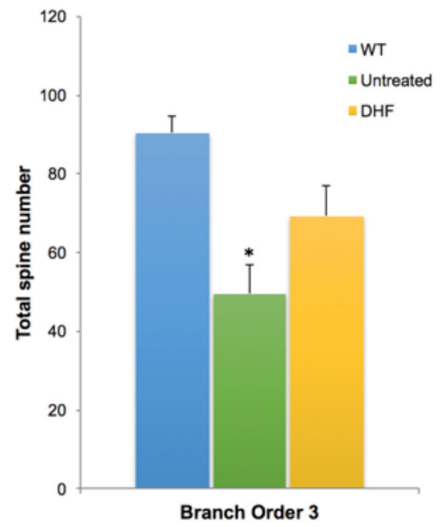
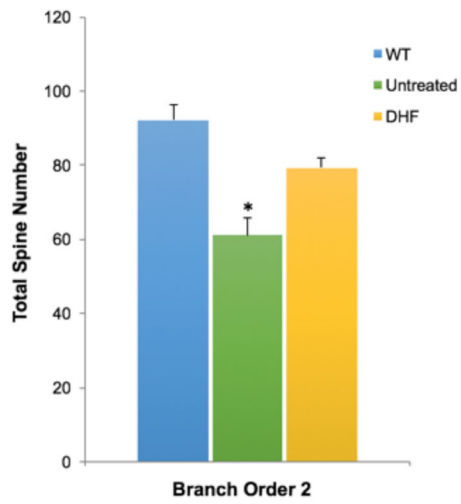
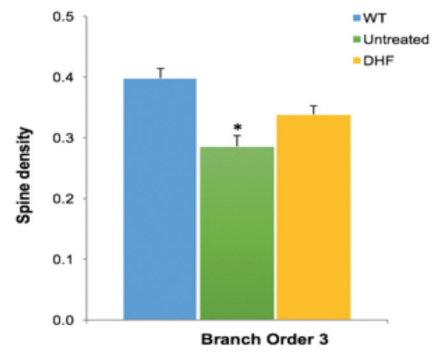
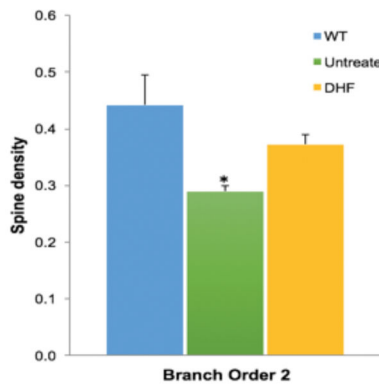
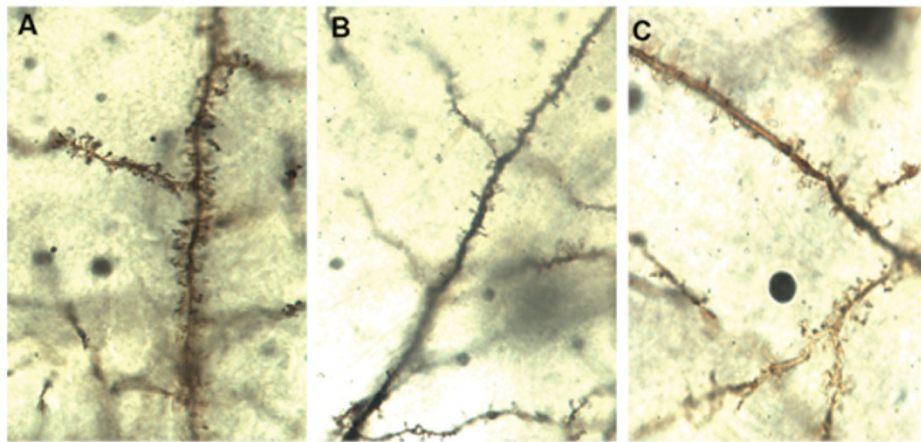


Fig 2. Representative micrographs and quantification analysis of the effect of 7,8-DHF (5mg/kg, i.p. injection / 3 days a week) on Aβ42 and 40 plaque burden of 3 month old 5xFAD mice that had been treated for 2 months. DHF treatment significantly reduced the Aβ42 plaque burden in 5xFAD mice (n=10) compared to the untreated 5xFAD mice (n=10) *P< 0.05. In contrast, Aβ40 plaque burden did not decrease significantly after 7,8-DHF treatment.



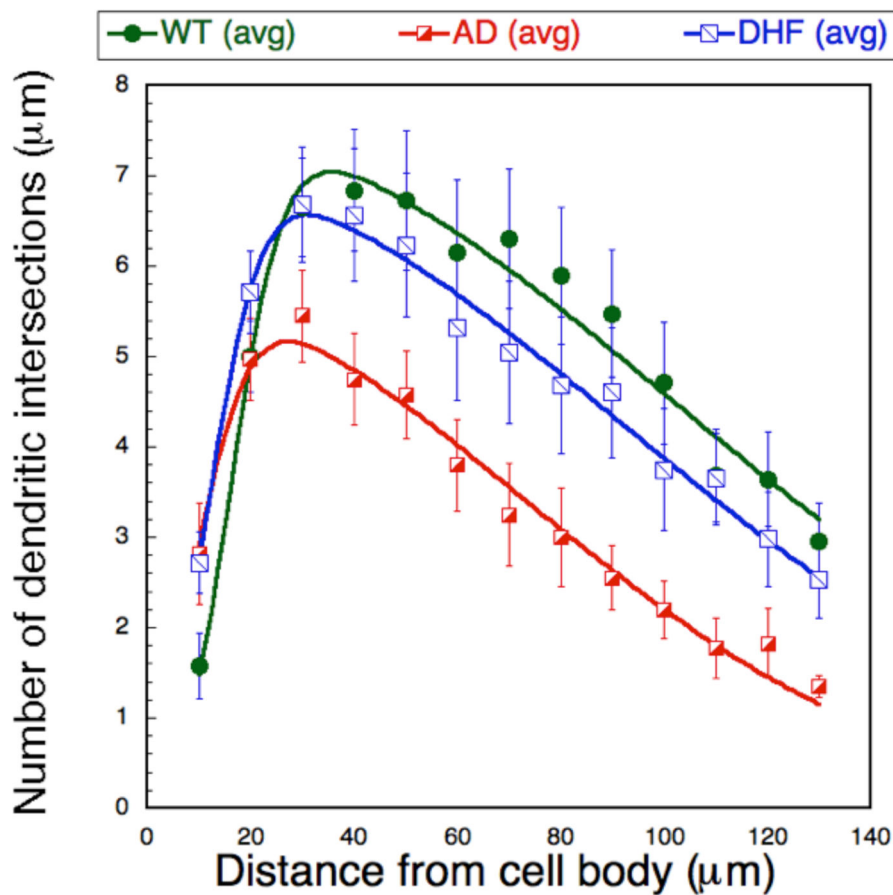


Fig 3.

Fig 3A. Spines on the dendritic branch of Golgi-stained neurons from WT (A), untreated (B), and 7,8-DHF- treated (C) experimental groups are shown (magnification 100x).

Fig 3B. Spine density was analyzed on order 2 and 3 dendritic branches of layer V cortical neurons in untreated WT, untreated 5xFAD and 7,8-DHF 5xFAD groups (n=10). Spine density was significantly lower in the untreated 5xFAD mice compared to WT mice.

However, spine density in the DHF-treated mice was not significantly different than that in WT mice. *P< 0.05.

Fig 3C. Total spine number on branch order 2 and 3 in untreated WT, untreated 5xFAD and 7,8-DHF 5xFAD treated groups of Layer V cortical neurons. The total number of spines in the untreated 5xFAD group (n=10) significantly decreased compared to the WT group (n=10); *P< 0.05. DHF treatment prevented dendritic spine loss in 5xFAD mice, as the number of spines counted in the 5xFAD treated group (n=10) and WT (n=10) was not significantly different.

Fig 3D. The number of dendritic intersections at each radial distance from the soma for each neuron was counted and graphed as mean data per mouse treatment group within WT, untreated and 7,8-DHF treated groups. We performed a Sholl analysis to measure dendritic field density and structure changes between groups. Shown are the fits for the WT, 5xFAD and 5xFAD 7,8-DHF groups (n=10) using an asymmetric Gaussian lineshape. The curves fits were significantly different for 5xFAD vs. WT (P<0.05 using the R-factor ratio test). The

5xFAD 7,8-DHF curve approached significance compared to the 5xFAD curve ($P < 0.1$) but there was no difference between the WT and 7,8-DHF-treated 5xFAD curves.

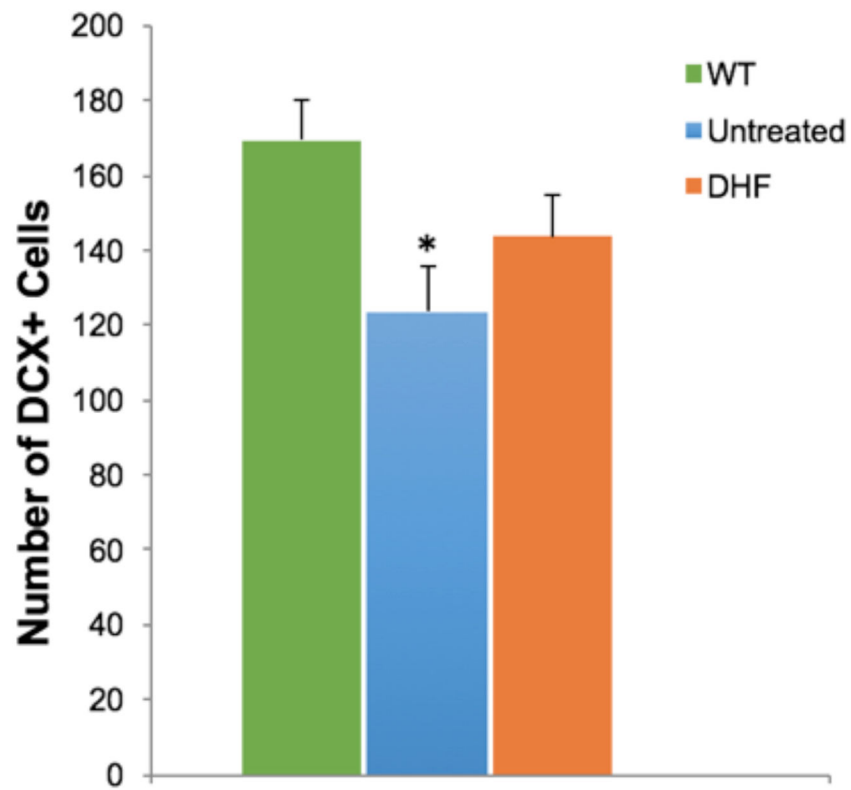


Fig 4.

Doublecortin (DCX) positive neurons of WT, untreated and 7,8-DHF treated 5xFAD mice in the dentate gyrus were quantified to analyze the effect of treatment on neurogenesis. Quantification was performed in 3 sections/mouse in 10 mice/group. Untreated 5xFAD mice had a significant reduction of DCX positive neurons compared to WT mice, however, DHF treatment did not reverse this decrease significantly; * $P < 0.05$.

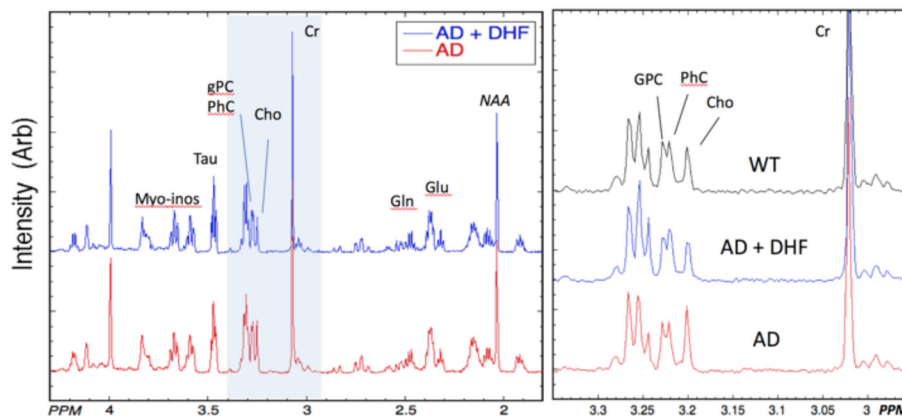


Fig 5. Left – ^1H HRMAS spectra averaged from all animals in each group of 5xFAD mice with (n=9) and without (n=8) 7,8-DHF supplementation. The spectra are normalized to the creatine (Cr) peak. The spectra are quite similar but increases in choline (Cho) can be seen in the 5xFAD spectrum compared to the 5xFAD + 7,8-DHF spectrum. Right – Expansions of three representative spectra from the “cholines” region (shown in blue on the left spectra) showing the increased Cho in the 5xFAD animal. These spectra were also normalized to the Cr peak. The separation between glycerophosphocholine (GPC) and phosphocholine (PhC) is small enough that it is blurred in the averaged spectra shown on the left, but is readily apparent in individual spectra.

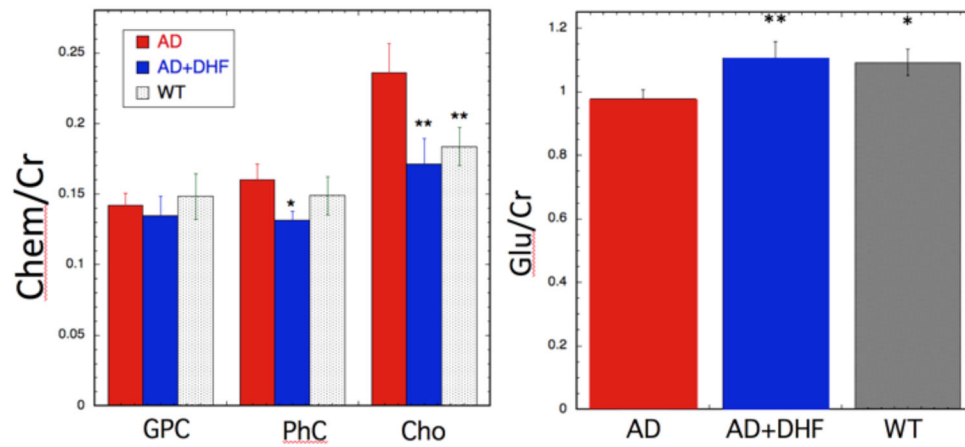


Fig 6.

Bar graphs for the neurochemicals that showed significant changes between the 5xFAD and 5xFAD +7,8-DHF animals. Left - Changes in the choline-containing chemicals glycerolphosphocholine (GPC), phosphocholine (PhC) and choline (Cho). 7,8-DHF treatment normalized the increases noted in PhC and Cho. Right – Glutamate levels in the hippocampus of WT, 5xFAD and 5xFAD+7,8-DHF treated mice showing the treatment effects of the DHF. **P<0.01 or * P < 0.05 for differences of the mean compared to the 5xFAD animals.